Efficient watt-level 0.775 µm SHG and 3.3 µm DFG in annealed and reverse proton exchanged diced PPLN ridge waveguides

Sergiy Suntsov[1,*], *Kore* Hasse[1], and *Detlef* Kip[1]

[1]Faculty of Electrical Engineering, Helmut Schmidt University, 22043 Hamburg, Germany

Abstract. We report on the fabrication of ridge waveguides formed in congruent periodically poled lithium niobate (PPLN). The waveguides were fabricated by periodic poling, proton exchange, subsequent annealing and reverse proton exchange followed by diamond blade dicing. Up to 1 W of single-pass second-harmonic generation at 775 nm has been realized in 50 mm long ridge waveguides with internal conversion efficiency of 70%. Furthermore, difference frequency generation at 3.3 µm of two pump waves at 1.05 µm and 1.55 µm has been obtained in similarly fabricated PPLN ridge waveguides with an appropriate poling period.

1 Introduction

Wide transparency window, excellent electro-optical, acousto-optical and nonlinear properties combined with low-loss waveguides make lithium niobate a material of choice for a wide variety of photonics applications. Due to large $\chi^{(2)}$ nonlinear coefficients and the possibility of controlled domain inversion on a micrometer scale, PPLN waveguide nonlinear frequency converters are used in optical telecommunications, for generation of squeezed states and entangled photon-pairs, laser cooling of atoms, and supercontinuum generation. Regarding frequency doubling of 1550 nm light, impressive peak conversion efficiencies of up to 4600 %/W have been reported [1, 2]. On the other hand, watt-level second-harmonic generation (SHG) outputs, have been demonstrated in PPLN waveguides with relatively low efficiencies of (50 – 100) %/W [3, 4]. PPLN waveguides both with channel and ridge geometries, have been also used for generation of mid-infrared (MIR) light in the (3.2 – 4) µm wavelength range through difference frequency generation (DFG) of the two pump waves with wavelengths around 1050 nm and 1550 nm. In different waveguide types, DFG efficiencies up to 70 %/W in the up to 8 cm long PPLN waveguides have been demonstrated [5, 6].

In this work, we report on the first annealed/reverse proton exchanged, diamond blade diced PPLN ridge waveguides with 510 %/W (25 %/W·cm^2) conversion efficiency. In high pump power regime, up to 1 W of SHG at 775 nm at 70 % pump power conversion is obtained [7]. Furthermore, DFG in the mid-infrared range around 3.3 µm is demonstrated in similarly fabricated PPLN ridge waveguides under 1.05 µm and 1.55 µm pumping.

2 Sample fabrication

The PPLN ridge waveguide fabrication process comprises four main steps: electric field poling of a $LiNbO_3$ substrate, proton exchange with subsequent annealing (APE), reverse proton exchange (RPE) and ridge waveguide definition. As a sample substrate, 50 mm long pieces of an optical-grade z-cut $LiNbO_3$ wafer were taken. First, electric field poling with a quasi-phase-matching (QPM) period of 18.2 µm for SHG and 26.6 µm for DFG over 45 mm length was conducted. The samples were proton exchanged for 100 minutes (SHG) or 5 hours (DFG) in pure benzoic acid melt at 200 °C, and then annealed in air for 18 hours at 350 °C. These particular proton exchange times were chosen in order to obtain (after annealing and RPE steps) single mode waveguides at 1.55 µm and up to 4 µm wavelengths for SHG and DFG samples, respectively. The in-depth refractive index (RI) profiles at 532 nm of the obtained planar waveguides for SHG after annealing were reconstructed based on the effective RIs of guided TM modes measured with a prism coupler.

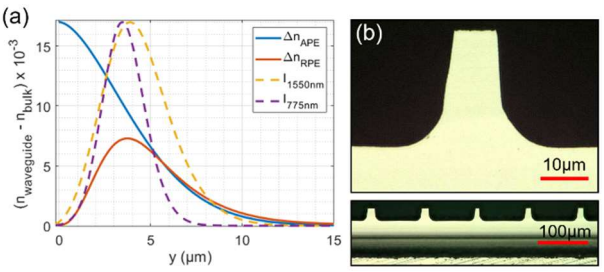

Fig. 1. (a) In-depth RI of measured APE (blue) and calculated RPE (red) planar waveguides at 532 nm. Dashed curves are simulated intensities of the fundamental modes after RPE at 1550 nm (yellow) and at 775 nm (violet). (b) Micro-graphs of the sample's facet at 500x and 2000x magnification.

* Corresponding author: suntsov@hsu-hh.de

The half-bell-shaped RI of the SHG sample is shown in Fig. 1 (a) with a blue curve and has a maximum increase of 0.017 at the surface with 4.0 µm width at 50 % height. The corresponding parameters of the fabricated DFG sample were found to be 0.038 and 3.5 µm. A subsequent RPE step was conducted in a Li-rich eutectic melt of $LiNO_3$:KNO_3:$NaNO_3$ for (5 – 7) hours at 330 °C. The RI profile after the RPE step is also shown in Fig. 1 (a). The simulated in-depth mode intensities of the RPE planar waveguide for SHG are shown with dashed lines in Fig. 1 (a). After RPE the guided modes are pushed away from the surface layer with damaged nonlinearity, and at the same time the more symmetric RI profiles lead to a significantly improved modes' overlap. Both effects are advantageous for efficient SHG. In the last step, ridges with widths (7 – 18) µm and a height of 25 µm were cut using a precision wafer saw (Disco DAD322), see micrographs of Fig. 1 (b).

3 Measurements setup

A schematic of the experimental setup for SHG measurements in our RPE PPLN ridge waveguides is presented in Fig. 2. The low power sub-milliwatt output of a fiber-coupled tunable laser source (New Focus Venturi TLB 6600 H CL) was amplified by a polarization maintained Er-doped fiber amplifier (EDFA, Keopsys CEFA-C-PM-HP-37) with an output power of up to 4.5 W. A collimator and an aspheric lens combination was used to inject the pump light into the waveguides. To facilitate coupling optimization, the in-coupling optics was mounted on a 3-axis piezo positioning system (Thorlabs Nanomax MAX341) with an auto-align option for tracking the output SH maximum (or throughput pump power maximum, when needed). The waveguide chip was placed inside an oven (Covesion PV50) for operation at elevated temperature. The second harmonic and the residual pump exiting the sample were collected and collimated with another aspheric lens. A beam sampler (BS) on a flip mount was used to reflect a small part of the output onto an infrared CCD camera while an appropriate filter (F, Thorlabs FGL1000M or Thorlabs FGB25) was inserted to separately record intensities of the pump and SH waveguide modes. The SH and the pump beams were then split in a short-pass dichroic mirror with 950 nm cut-off wavelength (DM, Thorlabs DMSP950) and their powers measured with calibrated Si and Ge high-sensitivity power sensors, respectively. To prevent sensors' saturation at higher power levels, neutral density filters as well as cross-check with a thermal power meter head were used. Furthermore, since the dichroic mirror has 2.5 % reflectance at 775 nm, and Ge sensor has non-negligible sensitivity at this wavelength, a long-pass filter (F1, Thorlabs FGL1000M) was used in front of the Ge power sensor to block the reflected second harmonic light. By determining the SHG and the residual pump powers at the waveguide's output, we accounted for the losses caused by the downstream optical components. To record the SHG and residual pump tuning curves, a swept-wavelength option of our laser and a digital oscilloscope were used.

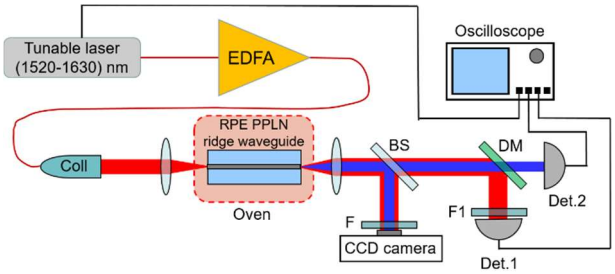

Fig. 2. Experimental setup for SHG characterization of RPE PPLN ridge waveguides. EDFA: erbium-doped fiber amplifier, Coll: collimator, BS: beam sampler, F, F1: filters, DM: short-pass dichroic mirror, Det.1 and Det.2: germanium and silicon power meters, respectively.

The setup for the DFG experiments (not shown) has an additional pump laser source at around 1050 nm (Sacher Lasertechnik Lion) with an output power of up to 400 mW. The two pump beams were combined in a dichroic mirror (Thorlabs DMSP1180). On the output side, the residual pumps were filtered out with a germanium filter, and the power of the generated MIR wave was measured with a mid-infrared detector (Hamamatsu P4631). Also, to record the intensity of the MIR waveguide modes an appropriate infrared camera (DataRay WinCamD-IR-BB) was used.

4 Experimental results

4.1 Second-harmonic generation

To reduce photorefractive damage (PRD) effects, during SHG experiment the sample's temperature was maintained at 120 °C. The recorded intensities of the pump and SH waveguide modes are shown in Fig. 3 (a). The measured low-power SHG tuning curve and the respective theoretical one, plotted in Fig. 3 (b), are in good agreement with a FWHM of 0.22 nm. We define the peak SHG conversion efficiency as $\eta = 100\ \%\cdot P_{SH}/(P_{p\text{-}in})^2$, where P_{SH} and $P_{p\text{-}in}$ are the exiting SH power and the pump power coupled into waveguide, respectively. From the parabola fit to the measured low-power dependence of P_{SH} on $P_{p\text{-}in}$ at QPM wavelength 1551.4 nm (inset of Fig. 3 (b)) a conversion efficiency of η = 510 %/W was extracted.

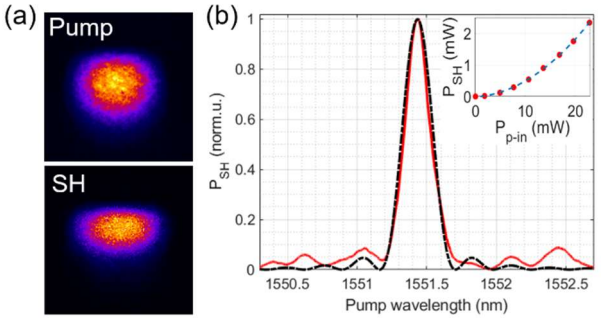

Fig. 3. (a) Recorded pump and SH mode intensities of the 10 µm wide RPE PPLN ridge waveguide (b) Measured (red solid) and calculated (black dashed) SHG tuning curve. Inset: low power P_{SH} vs. $P_{p\text{-}in}$ (circles) with a parabola fit (dashed).

P_{SH} and pump conversion efficiency into SH wave, defined as $\eta_{SHG} = 100\ \%\cdot P_{SH}/P_{p\text{-}in}$, vs. $P_{p\text{-}in}$ are plotted in

Fig. 4 (a). After the initial parabolic increase in the low pump depletion regime, a quasi-linear increase of P_{SH} was observed, and at $P_{p\text{-}in}$ = 1.2 W, the maximum $\eta_{SHG} \approx 70$ % was reached with 0.85 W of the SH output.

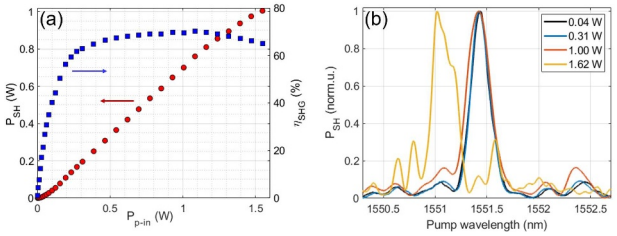

Fig. 4. (a) P_{SH} (circles) and η_{SHG} (squares) versus $P_{p\text{-}in}$. (b) SHG tuning curves for different coupled pump powers $P_{p\text{-}in}$.

With further $P_{p\text{-}in}$ increase, sub-linear P_{SH} grows and η_{SHG} decline were observed. The explanation for this behavior can be found in Fig. 4 (b) where the measured SHG tuning curves at different $P_{p\text{-}in}$ are shown. The observed blue shift of the spectral peak at $P_{p\text{-}in} > 1$ W clearly indicates PRD caused by the growing SH wave.

3.2 Difference frequency generation

Due to 3 times longer proton exchange time, ridge waveguides of our DFG PPLN sample supported the fundamental mode at up to 4 µm wavelength. To generate MIR light at a wavelength around 3.3 µm, a fixed pump at 1050 nm (Pump1) and a tunable pump in the (1520 – 1630) nm range (Pump2) were used. Figure 4 (a) shows the recorded modes of a 13 µm wide waveguide. For this ridge, the QPM was obtained at Pump2 wavelength of 1540 nm with the generated DFG wave at 3.3 µm.

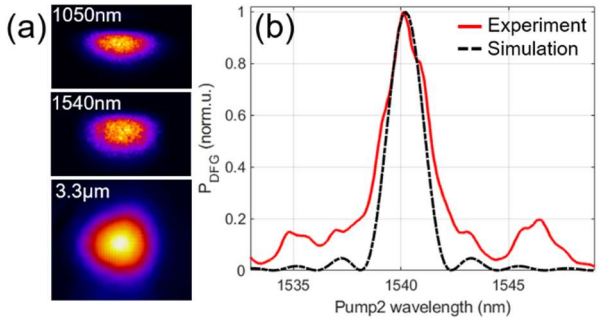

Fig. 4. (a) Experimentally measured Pump1, Pump2 and DFG mode intensities of the 13µm wide RPE PPLN ridge waveguide (b) Measured and simulated DFG tuning curves.

The measured and simulated DFG QPM tuning curves are presented in Fig. 4 (b). There is a clear deviation from the ideal $Sinc^2$ behavior caused by the imperfections in the fabrication process. Also, the experimental QPM peak is broader than the simulated one. The peak DFG conversion efficiency was found to be 3.2 %/W, which is an order of magnitude lower than the theoretical prediction. These discrepancies could be attributed to much higher propagation losses at 3.3 µm caused by OH^- absorption in proton-exchanged $LiNbO_3$ material and are currently under investigation.

4 Conclusion

To conclude, we have fabricated PPLN ridge waveguides using annealed and reverse proton exchange with subsequent diamond blade dicing. We reached the highest SHG power of 1 W at 775.7 nm and the internal conversion efficiency of 70 % reported to date for this type of PPLN waveguides. The maximum attainable SHG power is limited by PRD. Thus, PRD resistant substrates are needed for even higher power operation. In the RPE PPLN waveguides for mid-infrared DFG at 3.3 µm relatively low conversion efficiency was obtained that could be improved by shifting the DFG wavelength toward 4 µm, further away from the OH^- absorption peak.

Funding by Deutsche Forschungsgemeinschaft (DFG) (Ki482/17-1) is gratefully acknowledged.

References

1. T. Umeki, O. Tadanaga, and M. Asobe, IEEE J. Quantum Electron. **46**(8), 1206–1213 (2010).
2. R. Kou, S. Kurimura, K. Kikuchi, A. Terasaki, H. Nakajima, K. Kondou, J. Ichikawa, Opt. Express **19**(12), 11867 (2011)
3. C.-W. Hsu, R. Lai, C.-S. Hsu, Y.-T. Huang, K. Wu, M.-H. Chou, Proc. SPIE **10902**, 12 (2019)
4. L. G. Carpenter, S. A. Berry, A. C. Gray, J. C. Gates, P. G. R. Smith, C. B. E. Gawith, Opt. Express **28**, 21382–21390 (2020)
5. W. Denzer, G. Hancock, A. Hutchinson, M. Munday, R. Peverall, and G. A. D. Ritchie, Appl. Phys. B **86**, 437–442 (2007)
6. K.-D. F. Büchter, H. Herrmann, C. Langrock, M. M. Fejer, and W. Sohler, Opt. Lett. **34**, 470–472 (2009)
7. S. Suntsov, C. E. Rüter, D. Brüske, D. Kip, Opt. Express **29**, 11386 (2021)